

A computational dynamic analysis of sustainable electric vehicle fast charging station

Marcel A. A. Viegas*. Carlos Tavares da C., Jr.**

**Institute of Technology, Federal University of Para, PA, Brazil (e-mail: marcelviegas@ufpa.br).*

** *Institute of Technology, Federal University of Para, PA, Brazil (e-mail: cartav.ufpa@gmail.com)*

Abstract: This paper proposes the design and dynamic analysis of a possible topology of Electric Vehicle Fast Charging Station (EVFCS), which interconnects Photovoltaic Generator (PV); Stationary Batteries (SB); DC Bus; Electric Vehicle (EV); Power Switches; DC-DC Power Converters (Buck, Boost, and Bidirectional DC-DC Converter); Bidirectional AC-DC Converter; High Frequency Transformer (HFT); Matrix Converter (MC) and LCL Filter, with the possibility of connecting to the Utility Grid. The Stationary Battery will be charged slowly through the Photovoltaic System in the morning and afternoon hours and by the Utility Grid at night. Later, the Stationary Batteries will be discharged and will charge the Electric Vehicle Battery quickly (about 20-30 minutes) through a Bidirectional DC-DC Converter and through the Utility Grid, but with an effort much less to process high power in short time intervals in the distribution transformers. The power and control projects of the system were performed through calculations and validated by performing simulations. The simulations will be done in MATLAB / Simulink software. Three operating scenarios will be created, where the use or not of the Utility Grid will be analyzed, according to the intermittent of the Photovoltaic Generator, the State-of-Charge (SOC) of the Stationary Batteries and the Electric Vehicle. For this, there will be the management of the power flows that will be performed by Power Switches. The results indicate the effectiveness of the proposed strategies.

Resumo: Este artigo propõe o projeto e a análise dinâmica de uma possível topologia de Estação de Carregamento Rápido de Veículos Elétricos (ECRVE), que interconecta o Gerador Fotovoltaico (FV); Baterias Estacionárias (BE); Barramento CC; Veículo elétrico (VE); Chaves de Potência; Conversores de Potência CC-CC (*Buck*, *Boost* e Conversor CC-CC Bidirecional em Corrente); Conversor CA-CC Bidirecional; Transformador de Alta Frequência (TAF); Conversor Matricial (CM) e filtro LCL, com a possibilidade de conexão à Rede Elétrica. A Bateria Estacionária será carregada lentamente pelo Gerador Fotovoltaico no período matutino e vespertino e pela Rede Elétrica da concessionária à noite. Posteriormente, as Baterias Estacionárias serão descarregadas e carregarão a bateria do Veículo Elétrico de forma rápida (cerca de 20 a 30 minutos) através de um Conversor CC-CC Bidirecional em corrente e da Rede Elétrica, mas com um esforço muito menor para processar altas potências em curtos intervalos de tempo nos transformadores de distribuição. Os projetos de potência e controle do sistema foram realizados por meio de cálculos e validados por meio de simulações. As simulações serão feitas no software MATLAB/*Simulink*. Serão criados 3 cenários operacionais, nos quais será analisado o uso ou não da Rede Elétrica, de acordo com a intermitência do Gerador Fotovoltaico, o Estado de Carga (SOC) das Baterias estacionárias e do Veículo Elétrico. Para isso, haverá o gerenciamento dos fluxos de energia que serão executados pelas Chaves de Potência. Os resultados indicam a eficácia da estratégia proposta.

Keywords: Electric Vehicle Fast Charging Station, Photovoltaic Generator, Stationary Batteries, Power Converters.

Palavras-chaves: Estação de Carregamento Rápido de Veículos Elétricos, Gerador Fotovoltaico, Baterias Estacionárias, Conversores de Potência .

1. INTRODUCTION

The interest of many researchers has increased in Electric Vehicles (EVs), especially Plug-in Electric Vehicles (PEVs),

due to their flexibility, as these EVs can be used as loads, small generators or storage systems. In addition to providing lower pollutant emissions the Electric Vehicle also provides greater energy efficiency as it typically uses between 0.15 and 0.17 kWh per kilometer, while the average equivalent

consumption for a conventional vehicle with a consumption of 10 liters/100 km. It is 0.9 kWh per kilometer, thus proving that EV is significantly more efficient (Pang, Dutta and Kezunovic, 2011).

Electric Vehicles are gaining ground on the streets and roads. Most popular are Plug-in Hybrid Electric Vehicles (PHEV) and then purely electric (Plug-in Electric Vehicle - PEV). Today's PEVs feature autonomy, proportional to technology and battery size, between 150 km to 500 km for a charge. Although, the average daily use of each driver is around 50 km (Boulanger et al., 2011). In recent years, more than 2 million EVs have been sold worldwide. Countries such as China, the United States and Japan, are the ones that lead in number of sales. The production of electric vehicles is increasing and it is estimated that by 2025 electric cars already represent 15% of the world market; today, they are only 0.86%, according to the *International Energy Agency* (2017).

Several papers have been published recently, with proposals for Electric Vehicle Fast Charging Stations. In Savio et al. (2019), a Microgrid Energy Management System dedicated to charging Electric Vehicles is proposed consisting of: Photovoltaic Generator, Stationary Batteries, Bidirectional DC-DC and AC-DC Converters, and possibility of connection to the Utility Grid. The proposed system aims to minimize the effort of using the Utility Grid to charge Electric Vehicles by controlling the power flows between the components of the Microgrid.

In Hassoune et al. (2018), a Photovoltaic Generator Fast Charging Station, Stationary Battery, and Utility Grid topology is studied through a Bidirectional AC-DC converter and DC Bus implemented in the MATLAB / Simulink software. In Ballen et al. (2018), the design of a Fast Charging Station with energy storage element and active harmonic filter for Electric Vehicles is made, without the use of renewable sources, using only the Utility Grid and Stationary Batteries for the purpose of charging.

In Waltrich (2012), a 40 kW station prototype was designed that adds Stationary Batteries, Bidirectional DC-DC and AC-DC Converter, High Frequency Transformer, Matrix Converter and Power Grid connection, without the use of renewable sources and no power flow management.

Based on the above discussion, this paper presents possible standard for a Sustainable and Intelligent Electric Vehicle Fast Charging Station, with a topology that allows interconnection: Photovoltaic Generator (PV); Stationary Batteries (SB); Utility Grid; DC bus; Electric Vehicle; power switches; DC-DC converters (Buck, Boost, and Bidirectional DC-DC Converter); Bidirectional AC-DC converter; High Frequency Transformer; Matrix Converter and LCL Filter, as shown in Fig. 1.

This paper is structured as follows. Section 2 presents the principal components of the proposed Electric Vehicle Fast Charging Station. Section 3 presents simulation results for validation of the building blocks of the EVFCS operating together. The main conclusions are addressed in Section 4.

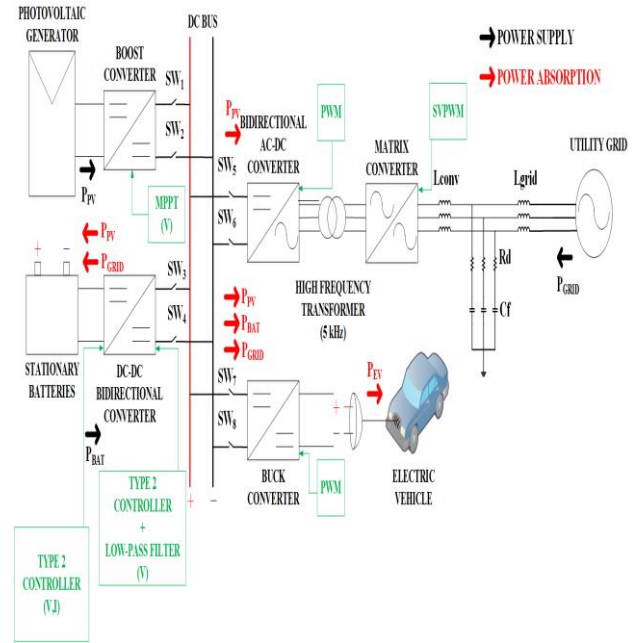


Fig. 1. Electric Vehicle Fast Charging Station proposed.

2. ELECTRIC VEHICLE FAST CHARGING STATION

In this paper, we design and simulate the entire system schematized in Fig. 1, proposing the control of all power flows. Non-isolated DC-DC power converters (Buck, Boost, and Bidirectional DC-DC Converter) and Bidirectional AC-DC Converter are used. So much so that the Photovoltaic Generator (preferably) and the Utility Grid will slowly charge the Stationary Battery Bank. The first will be charged during periods of higher system productivity, that is, during the day and in the afternoon, and the second will be charged at night.

The Stationary Batteries via the Bidirectional DC-DC Converter will quickly charge the battery of the Electric Vehicle in the EVFCS, and the Utility Grid may or may not contribute to this quick charge depending on the Power State. Stationary Battery Bank charge, the time of day and the operating conditions of the distribution transformer. The management of power flows in the Microgrid (MG) under study will be performed by power switches that will prevent, for example, reverse flows.

Electric Vehicle charging technologies are under constant development and research. The chargers of these vehicles may operate on AC or DC according to the characteristics of the charging method used (1 to 3) recommended by the Society for Automotive Engineers (SAE J1772, 2010).

The AC Level 1 method is very common in residential and small commercial buildings, the AC Level 2 method is used in both small and large residential and commercial environments, whether private or public, such as charging stations, shopping centers, work environments, etc. The AC Level 3 method is still under development. The DC method already exists at two levels: DC Level 1 and DC Level 2 and are preferably used in fast charging stations, DC Level 3 method is under development. The method employed in this paper, aiming at fast charging, will be DC Level 2, because it is the method that best fits the Brazilian distribution grid

voltage standards. With DC bus voltage regulated at $400\text{ V} \pm 10\%$ and currents of the order of up to 200 A .

All components of the system were initially designed and simulated separately to validate their proper functioning, and then linked together. For this, we used the *Simpowersystems* tool associated with *Simulink*® that comes with the *MATLAB*® software, whose version was 2016a.

2.1 PV Simulink Model

The PV Generator and its respective DC-DC Boost Converter whose parameters are: $R_{boost} = 5\text{ m}\Omega$; $L_{boost} = 5\text{ mH}$; $C_{PV} = 80\text{ }\mu\text{F}$; $C_{DC\text{ Bus}} = 256\text{ mF}$; $D = 0.5$; 10% current ripple, 1% voltage ripple, for coupling to DC Bus which is emulated by a capacitance whose maximum allowable voltage value is 1500 VDC , together with the Maximum Power Point Tracking Controller (MPPT), is shown in Fig. 2.

To obtain the maximum power from the solar panels, an efficient tracker algorithm is required for the MPPT. The tracker algorithm's task is to track the maximum power point of the solar panel is Incremental Conductance (IC) algorithm (El-Shahat and Sumaiya, 2019). The photovoltaic modules used are Canadian Solar polycrystalline silicon, model CS6X-310P, whose datasheet are see in https://www.canadiansolar.com/downloads/datasheets/na/Canadian_Solar-Datasheet-CS6XPFPG_Diamond-v5.3_na.pdf.

The available area considered for the installation of photovoltaic panels is variable and depends on the space available for the projected charging station. In this study, it was considered that, on average, a typical station has a covered area of 250 m^2 (Savio et al., 2019). To cover the available area of about 250 m^2 , it is necessary to install 7 modules in series and 16 strings in parallel of 7 modules associated in series, totaling an area of 214.9 m^2 for the Photovoltaic Generator equivalent. The Equivalent PV Generator project specifications are: $P_{mpp} = 34734.3\text{ W}$; $V_{oc} = 314.3\text{ V}$; $I_{sc} = 145.28\text{ A}$; $V_{mpp} = 254.8\text{ V}$; $I_{mpp} = 136.32\text{ A}$; $Width = 13.678\text{ m}$; $Length = 15.712\text{ m}$; $Area = 214.9\text{ m}^2$. Fig. 3 shows the I-V and P-V curves of the designed Photovoltaic Generator.

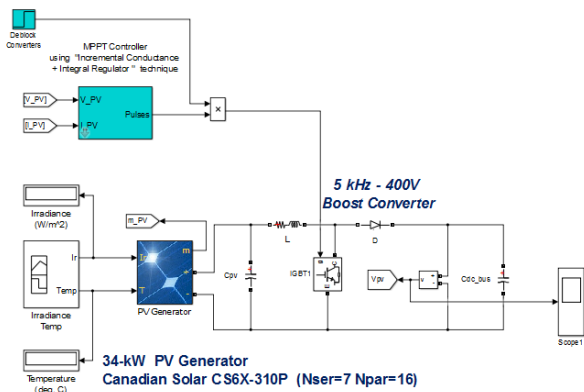


Fig.2. PV Generator, MPPT Controller and Boost Converter.

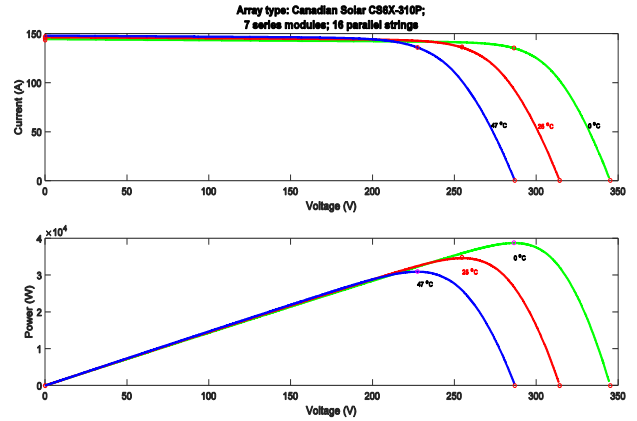


Fig.3. PV Generator I-V and P-V curves.

2.2 Stationary Batteries

The battery model used in the construction of the SB is the BYD B-PLUS 2.5 PRO 2.56 kWh 48 V LITHIUM 6.000 CYCLES, and you can consult its datasheet in <http://www.aldo.com.br/Produto/?c=39675&d=bateria-byd-aldos-olar-B-PLUS>. Since a $400\text{ VDC} \pm 10\%$ bus voltage is required, a SB must be used to increase the voltage value supplied to the Bidirectional DC-DC Converter connecting the battery system to the bus. By combining 8 batteries in series, a voltage of $V_{SB} = 8 \times 48 = 384\text{ V}$ is reached, and a nominal capacity of approximately 50 Ah , which already allows the use of a Boost converter and regulated in $400\text{ VDC} \pm 10\%$.

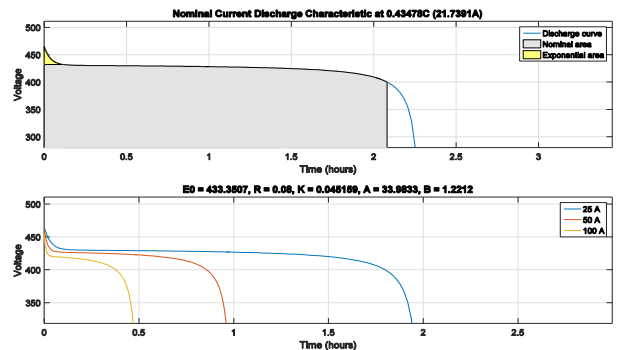


Fig.4. Stationary Batteries Discharge Curves at rated current and for certain current values.

2.3 Electric Vehicle and Buck Converter

The Plug-in Electric Vehicle chosen in this study for the simulations was full technical specifications are available at <https://www.nissanusa.com/ev/media/pdf/specs/FeaturesAndSpecs.pdf>. The battery has a Maximum Capacity of 24 kWh , and the Maximum Charging Time is $20\text{-}30\text{ min}$. at fast charge. Basically, the Electric Vehicle used in this study will be modeled as a Lithium-Ion Battery, whose manufacturer specifications are: Nominal capacity 56.3 Ah , 96 series cells associated with 3.65 V each, totaling a nominal voltage of 350.4 V .

The Buck converter whose parameters are: $R_{buck} = 0.1 \text{ m}\Omega$, $L_{buck} = 4.93 \text{ mH}$, $C_{buck} = 8.93 \text{ }\mu\text{F}$, $D = 0.5$, 10 % current ripple, 1 % voltage ripple; which regulates and lowers the DC bus voltage for the Electric Vehicle load, is also shown the converter scalar Pulse Width Modulation (PWM) control loop, whose parameters of the PI controller are: Proportional Gain (K_P) of 40, Integrative Gain (K_I) of 5000.

2.4 Bidirectional DC-DC Converter

The Bidirectional DC-DC Converter proposed in Fig. 5 is the device responsible for the process of charging and discharging the batteries, i.e. it's the system's Stationary Battery Charge Controller. The converter has two distinct operating steps, called Buck Stage (Stationary Batteries side) and Boost Stage (DC bus side).

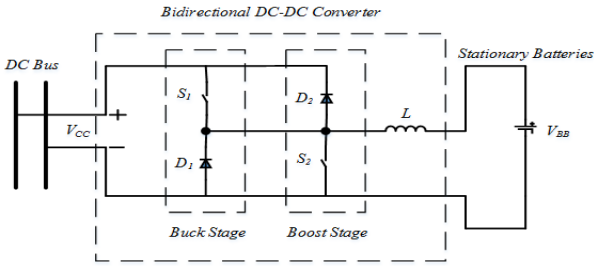


Fig.5. Proposed Topology of Bidirectional DC-DC Converter.

The converter transfer functions (Mohan, 2012) in Buck Stage are:

$$T_{vd1}(s) = \frac{\tilde{v}_{BB}(s)}{\tilde{d}(s)} = \frac{(r_B r_C C V_{CC})s + (r_B V_{CC})}{(r_B L C + r_C L C)s^2 + (r_B r_L C + r_B r_C C + r_C r_L C + L)s + (r_B + r_C)} \quad (1)$$

$$T_{id}(s) = \frac{\tilde{i}_L(s)}{\tilde{d}(s)} = \frac{C V_{CC} (r_B + r_C)s + V_{CC}}{(r_B L C + r_C L C)s^2 + (r_B r_L C + r_B r_C C + r_C r_L C + L)s + (r_B + r_C)} \quad (2)$$

$$T_{vd2}(s) = \frac{\tilde{v}_{CC}(s)}{\tilde{d}(s)} = \frac{a_1 s^2 + a_2 s + a_3}{b_1 s^2 + b_2 s + b_3} \quad (3)$$

Where:

$$a_1 = -V_{BB} r_C R L C \quad (4)$$

$$a_2 = V_{BB} (r_C C R^2 - r_C L - R L - 2 r_C C R^2 D + D^2 r_C C R^2 - r_C r_L C R) \quad (5)$$

$$a_3 = V_{BB} (D^2 r_C R - 2 D r_C R - r_L R + r_C R + R^2 - 2 R^2 D + R^2 D^2 - r_C r_L) \quad (6)$$

$$b_1 = (r_C + r_L - D r_C R + R - 2 R D + R D^2) R L C \quad (7)$$

$$b_2 = (r_C + r_L - D r_C R + R - 2 R D + R D^2) (L + r_C C R + r_L C R - D r_C C R) \quad (8)$$

$$b_3 = (r_C + r_L - D r_C R + R - 2 R D + R D^2)^2 \quad (9)$$

The Bidirectional DC-DC Converter project specifications are: $V_{CC} = V_{BB} = V_{SB} = V_1 = V_2 = 400 \text{ V}$; $R = 8 \text{ }\Omega$; $f_s = 5 \text{ kHz}$; $D_{buck} = 0.44$; $D_{boost} = 0.56$; $L = 200 \text{ }\mu\text{H}$; $C_{high} = 65 \text{ }\mu\text{F}$; $C_{low} = 32.5 \text{ }\mu\text{F}$; $r_L = 0.025 \text{ }\Omega$; $r_C = 0.2 \text{ }\Omega$, $r_B = 0.8 \text{ }\Omega$.

The design parameters to be calculated for the Bidirectional DC-DC Converter, shown in El-Shahat and Sumaiya (2019) are basically the inductance L , the capacitance C_{low} that is under the same voltage as the DC bus, and the capacitance

C_{high} which is under the same voltage as the Stationary Batteries and are given by the following equations:

$$L = \frac{1}{2 f_s P} \left(\frac{1}{V_1} + \frac{1}{V_2} \right)^2 \quad (10)$$

$$C_{high} = \frac{\Delta I_L}{8 \Delta V_C} T_s \quad (11)$$

$$C_{low} = \frac{V_1 D}{\Delta V_C R_L} T_s \quad (12)$$

In the literature, the lowest capacitance C_{low} that is under the same voltage as the DC bus, because as a higher voltage value is desired, the capacitance is reduced to a value by twice less than C_{high} (El-Sharat and Sumaiya, 2019). The methodology adopted in the design of the voltage control feedback loop for the Bidirectional DC-DC Converter is based on the K factor developed by Venable (Biesecker et al., 2004). K Factor is a mathematical tool that enables the synthesis of control feedback loops through operational amplifiers to achieve the desired frequency crossover and phase margin.

The transfer function of the Type 2 compensator (Mohan, 2012) used for voltage and current compensation in Buck Stage are:

$$C(s) = \frac{A(s + \omega_z)}{s(s + \omega_p)} \quad (13)$$

where: ω_z is the frequency of the compensator zero and ω_p is the frequency of the compensator pole. A is the compensator gain and can be calculated by:

$$\omega_z = \frac{\omega_{CG}}{K} \quad (14)$$

$$\omega_p = K \omega_{CG} \quad (15)$$

$$A = \frac{\omega_z}{|G(s)|_{f=f_{CG}}} \quad (16)$$

where: $|G(s)|_{f=f_{CG}}$ is the magnitude of the transfer function at the gain frequency of the controller without compensation.

The parameters of Voltage Compensator for Buck Stage of Bidirectional DC-DC Converter are: $R_1 = 10 \text{ k}\Omega$; $R_2 = 354 \text{ }\Omega$; $C_1 = 3,98 \text{ }\mu\text{F}$; $C_2 = 32,83 \text{ nF}$; $A = 24,904$. Current Compensator parameters are: $R_1 = 10 \text{ k}\Omega$; $R_2 = 399,9 \text{ }\Omega$; $C_1 = 21,92 \text{ }\mu\text{F}$; $C_2 = 4,63 \text{ nF}$; $A = 4,56$. It was considered in the project $R_1 = 10 \text{ k}\Omega$. With this value, it is possible to calculate the capacitance C_1 and C_2 and resistance R_2 values. And can be calculated by:

$$C_2 = \frac{|G(j\omega_{CG})|}{K R_1 \omega_{CG}} \quad (17)$$

$$C_1 = C_2 (K^2 - 1) \quad (18)$$

$$R_2 = \frac{K}{C_1 \omega_{CG}} \quad (19)$$

The Boost Stage voltage control compensator, for simplicity-efficiency ratio (Mohan, 2012), was made via pole allocation with the *Sisotool*/MATLAB is shown in Fig. 6.

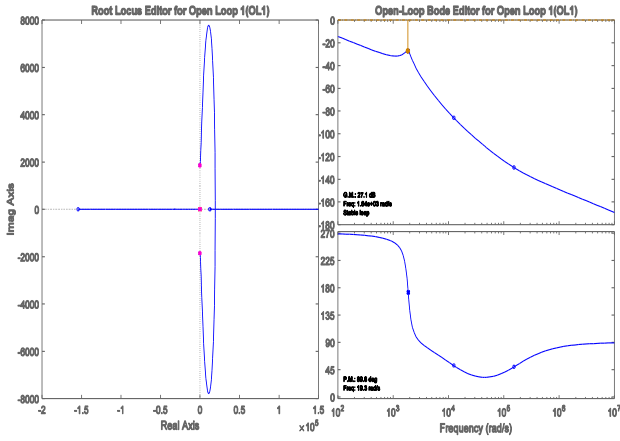


Fig. 6. Root Locus and Bode diagrams for Boost Stage $T_{vd1}(s)$ voltage controller, properly compensated via pole allocation in *Sisotool*.

2.5 Utility Grid

The simulated Utility Grid, in turn, was considered three-phase balanced with equally spaced 120° phasors, $254 V_{rms}$ phase-neutral voltage, $440 V_{rms}$ phase-phase voltage, followed by RL filters. Series resistance: $R_{Utility\ Grid} = 0.1 \Omega$ and series inductance: $L_{Utility\ Grid} = 500 \mu H$.

3. SIMULATION RESULTS

Three simulations of operating modes will be performed for the Microgrid under study: in Mode 1 the PV Generator supplies power to the Stationary Batteries (SB), the Electric Vehicle and the Utility Grid; in Mode 2 Stationary Batteries provide power to the EV; and in Mode 3 there is no photovoltaic generation available and the Power Grid supplies power to both Stationary and Electric Vehicle Batteries. The various Modes and power flows are as follows:

- (1) PV generator supplies SB, VE and Utility Grid (Mode 1);
- (2) SB provides power to the Electric Vehicle (Mode 2);
- (3) Utility Grid supplies SB and EV (Mode 3);

Mode 1: PV generator supplies to SB, EV and UG

In this operating scenario, the operating conditions are: the Electric Vehicle has a low State of Charge ($SOC_{EV} = 30\%$), the Stationary Battery has a low State of Charge also ($SOC_{SB} = 30\%$) and there is a good Irradiation condition ($700 W/m^2$) and temperature ($47^\circ C$), which would correspond, for example, to morning or afternoon charging. In such a way that the charging of the Stationary Batteries takes place preferably by the Photovoltaic Generator (around 2 h). The output voltage set on the DC Bus at $400 V \pm 10\%$ of the PV Generator plus Boost converter together with the regulated current of approximately $106 A$ applied to the DC Bus are shown in Fig. 7 and Fig. 8.

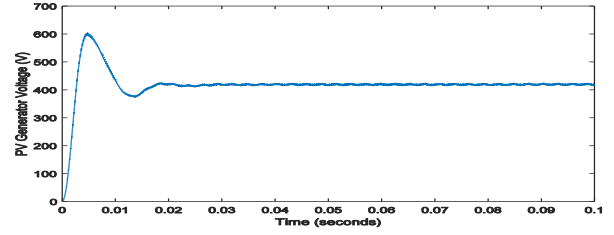


Fig. 7. PV Generator Voltage applied to DC Bus.

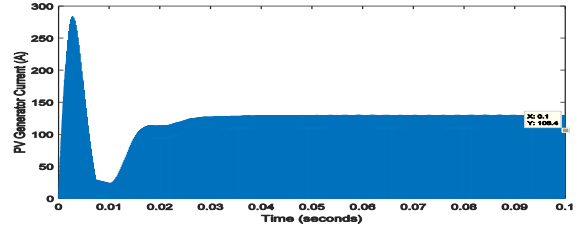


Fig. 8. PV Generator Current, output of Boost Converter applied to DC Bus in Mode 1.

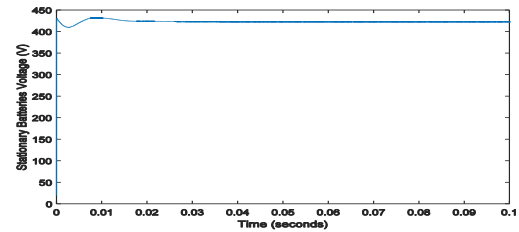


Fig. 9. Stationary Batteries Voltage during slow charging in Mode 1.

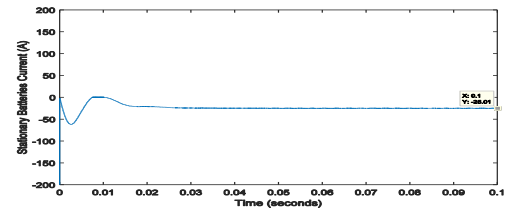


Fig. 10. Stationary Batteries Current during slow charging in Mode 1.

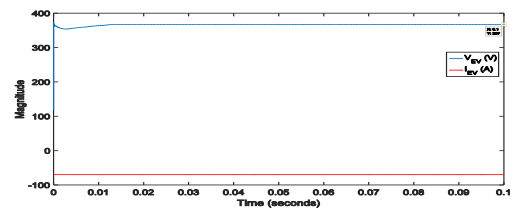


Fig. 11. EV Voltage and Current regulated during fast charging in Mode 1.

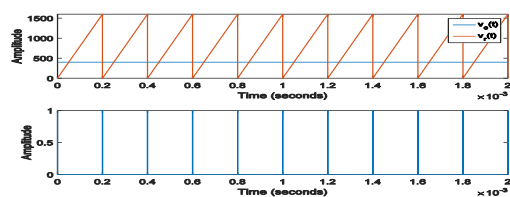


Fig. 12. PWM control applied in Buck Converter of EV charger.

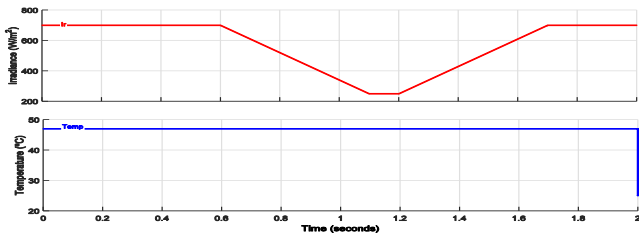


Fig. 13. Irradiance and Temperature of PV Generator in Mode 1.

Fig. 14 illustrates the Bidirectional AC-DC Converter output phase voltages applied to the High Frequency Transformer inputs. Fig. 15 shows the phase voltages of the High Frequency Transformer output at both $400\text{ V} \pm 10\%$ and 5 kHz frequency of 3 levels square wave, which will be applied to the inputs of the Matrix Converter that will convert the waveforms 254 V per phase and 60 Hz frequency that will be injected into the Utility Grid after filtering by the input LCL filter, as shown in Fig. 16, while in Fig. 17 are shown the phase currents injected into the Utility Grid with peak value 10 A and 60 Hz frequency after filtering.

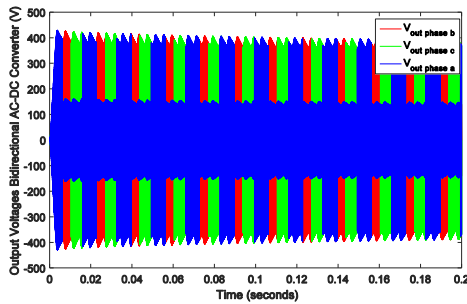


Fig. 14. Bidirectional AC-DC Converter output phase voltages.

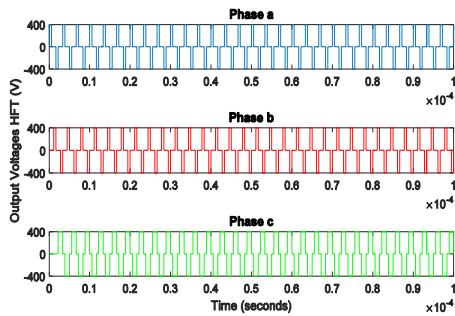


Fig. 15. Output phase voltages of the High Frequency Transformer.

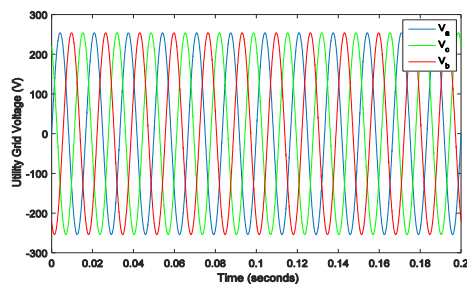


Fig. 16. Phase voltages injected into Utility Grid after filtering by LCL filter.

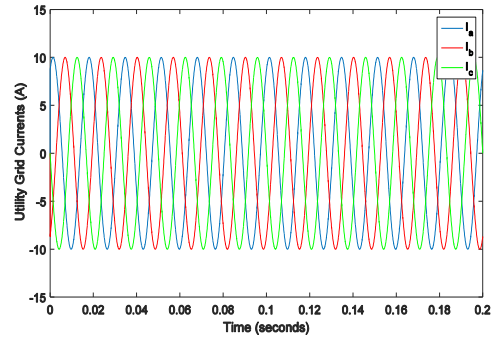


Fig. 17. Phase currents injected into the Utility Grid after filtering by LCL filter.

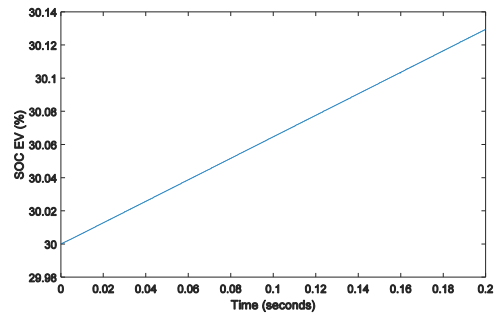


Fig. 18. SOC EV in fast charging process in Mode 1.

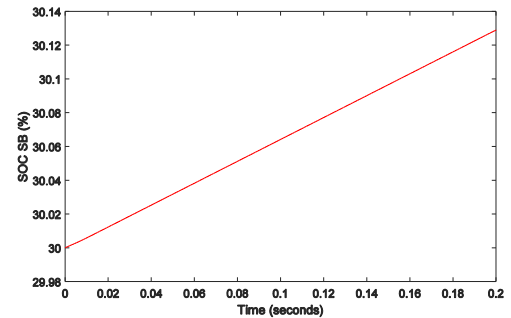


Fig. 19. SOC SB in slow charging process in Mode 1.

Mode 2: SB provides power to the Electric Vehicle

In this operating scenario, the conditions are: the Electric Vehicle has a low State of Charge ($SOC_{EV} = 20\%$), the Stationary Battery has a high State of Charge ($SOC_{SB} = 90\%$), there is no Solar Irradiation (0 W/m^2), and low temperature ($25\text{ }^\circ\text{C}$), which would correspond, for example, to a nightly charging and also simulate the unavailability of the Utility Grid.

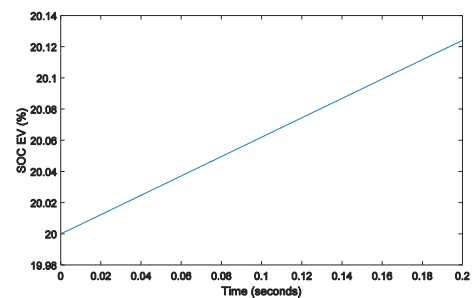


Fig. 20. SOC EV in fast charging process in Mode 2.

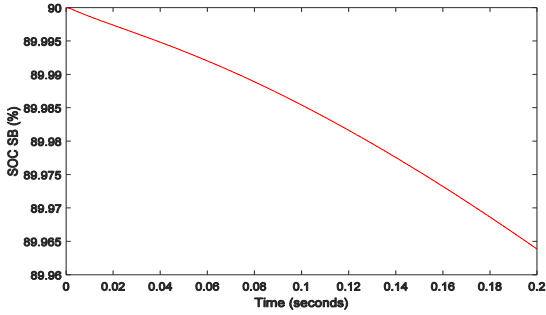


Fig. 21. SOC SB in fast discharging process in Mode 2.

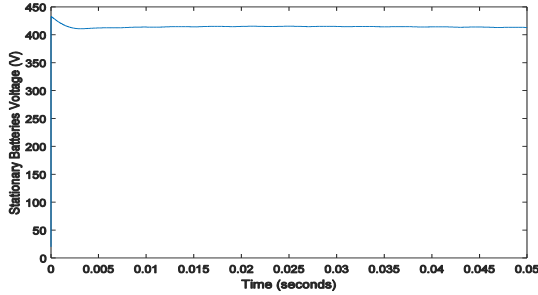


Fig. 22. Stationary Batteries Voltage during fast discharging in Mode 2.

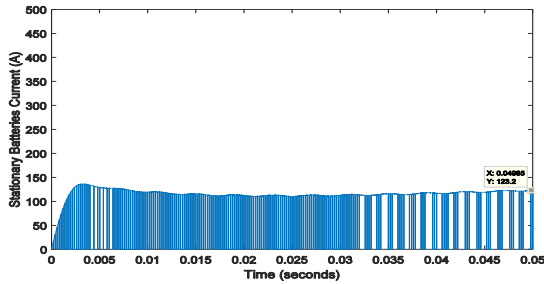


Fig. 23. Stationary Batteries Current, applied to DC Bus in Mode 2.

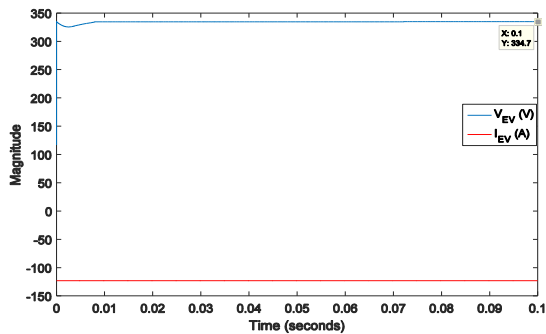


Fig. 24. EV Voltage and Current regulated during fast charging in Mode 2.

Mode 3: Utility Grid supplies to SB and EV

In this operating scenario, the operating conditions are: the Electric Vehicle has a low State of Charge ($SOC_{EV} = 40\%$), the Stationary Battery has a intermediate State of Charge also ($SOC_{SB} = 50\%$) there is no Solar Irradiation ($0 W/m^2$), and low temperature ($25\text{ }^\circ C$), which would correspond, for

example, to a nightly charging, but in this case, the Utility Grid will be responsible for the fast charging of the Electric Vehicle and the slow charging of the Stationary Batteries.

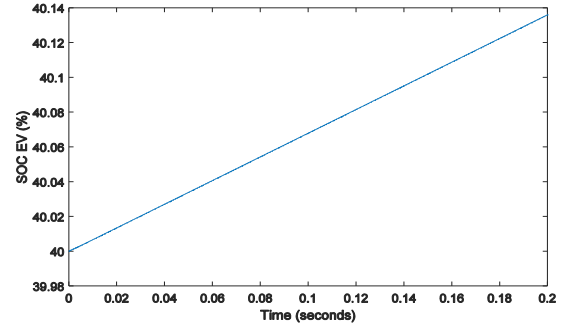


Fig. 25. SOC EV in fast charging process in Mode 3.

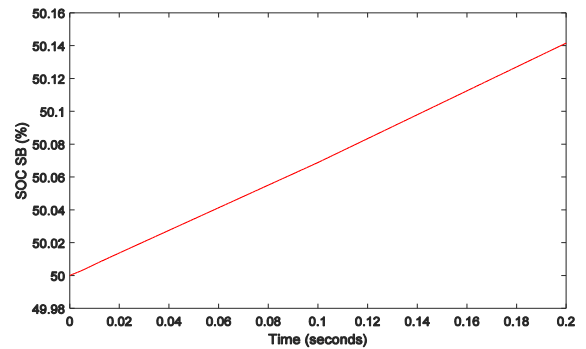


Fig. 26. SOC SB in slow charging process in Mode 3.

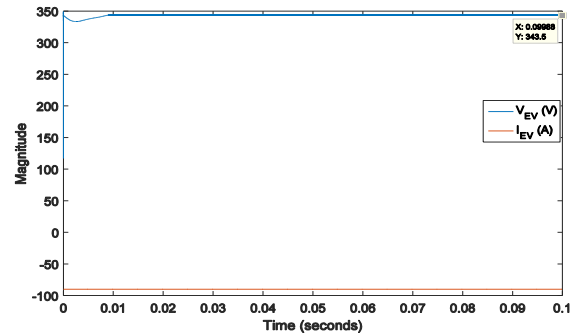


Fig. 27. EV Voltage and Current regulated during fast charging in Mode 3.

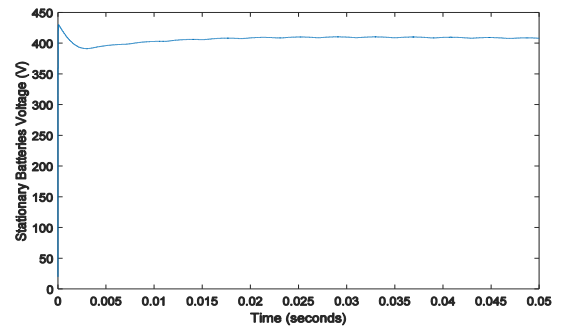


Fig. 28. Stationary Batteries Voltage during slow charging in Mode 3.

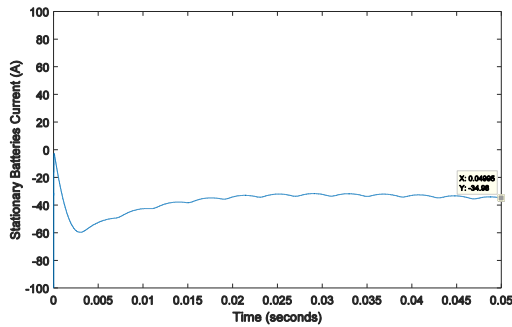


Fig. 29. Stationary Batteries Current during slow charging in Mode 3.

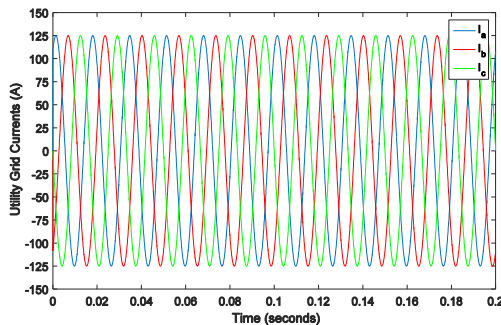


Fig. 30. Phase currents injected by Utility Grid in Matrix Converter in Mode 3.

4. CONCLUSION

This paper developed the design and dynamic analysis of a sustainable electric vehicles fast charging station. Different from other literature topologies, was implemented Space Vector Pulse Width Modulation (SVPWM) Control in Matrix Converter, a Bidirectional AC-DC Converter and a High Frequency Transformer (5 kHz) for the bidirectional power flow from the Utility Grid to the EVFCS and vice versa and aiming to inject as close as possible 60 Hz waveforms voltages and currents to the Utility Grid, proved by the results obtained to be an advantage over other topologies of literature. In addition, the use of the High Frequency Transformer allows galvanic isolation of the proposed Electric Vehicle Fast Charging Station in case of a power grid side failure. Another advantage is that the SVPWM control enables bidirectional mode power flow management and better use of the DC Bus. For this, 3 operating scenarios were analyzed, with the objective of validating by simulation the system that was designed. The intermittence of the photovoltaic generator, the unavailability of the Utility Grid and the State-Of-Charge of SB and EV.

REFERENCES

Balen, G., Reis, A. R., Pinheiro, H. and Schuch L (2018). Fast charger station with energy storage element and harmonics active filter for electric vehicles, SOBRAEP, February.

Biesecker, T. E (2004). Optimum Feedback Amplifier Design for Control Systems”, Venable Technical Paper #3, Venable Industries, www.venable.biz, August.

Boulanger, A.G., Chu, A.C., Maxx, S. and Waltz, D. L (2011). Vehicle Electrification: Status and Issues, Proceedings of the IEEE, vol. 99, no. 6, pp.1116–1138, June.

BYD B-PLUS Web Site [Online]. Available in: <http://www.aldo.com.br/Produto/?c=39675&d=bateria-byd-aldos-olar-B-PLUS>.

Canadian Solar Web Site [Online]. Available in: https://www.canadiansolar.com/downloads/datasheets/na/Canadian_Solar-Datasheet-CS6XPFG_Diamond-v5.3_na.pdf.

El-Shahat, A. and Sumaiya, S (2019). DC-Microgrid System Design, Control, and Analysis, Electronics Journal, MDPI, January.

Global EV Outlook (2017) – Two million and counting, InternationalEnergyAgency.

Hassoune, A., Khafallah, M., Mesbahi, A. and Bouragba T (2018). Power Management Strategies of Electric Vehicle Charging Station Based Grid Tied PV-Battery System, International Journal of Renewable Energy Research, June.

Mohan, N (2012). Power Electronics: A first course. LTC.

Nissan Leaf Web Site [Online]. Disponível em: <https://www.nissanusa.com/ev/media/pdf/specs/FeaturesAndSpecs.pdf>.

Pang, C.; Dutta P. and Kezunovic, M (2011). BEVs/PHEVs as Dispersed Energy Storage for V2B Uses in the Smart Grid, IEEE Transactions on Smart Grid, Special Issue on Transportation Electrification and Vehicle-to-Grid Applications.

SAE (2010). Recommended Practice for Electric Vehicle and Plug in Hybrid Electric Vehicle Conductive Charger Coupler, SAE Standard J1772.

Savio, D. A., Juliet, V. A., Chokkalingam, B., Padmanaban, S., Holm-Nielsen, J. B. and Blaabjerg, F (2019). Photovoltaic Integrated Hybrid Microgrid Structured Electric Vehicle Charging Station and Its Energy Management Approach, Energies, vol. 12.

Waltrich, G., Hendrix, M. and Duarte, J. L (2012). Power flow steering for electric vehicle fast charging station, Energy Conversion Congress and Exposition (ECCE), 2012 IEEE, September.